ISSN 1028-334X, Doklady Earth Sciences, 2022, Vol. 507, Part 2, pp. 1112–1117. © Pleiades Publishing, Ltd., 2022.
Russian Text © The Author(s), 2022, published in Doklady Rossiiskoi Akademii Nauk. Nauki o Zemle, 2022, Vol. 507, No. 2, pp. 309–315.

SEISMOLOGY

Study of the Features of Seismogenic Activation of the Chilean Subduction Zone at the Beginning of the 21st Century

I. S. Vladimirova[a,b,*]

Submitted by Academician L.I. Lobkovsky August 5, 2022

Received August 12, 2022; revised September 1, 2022; accepted September 7, 2022

Abstract—The analysis of seismotectonic deformations associated with the seismogenic activation of the Chilean subduction zone at the beginning of the 21st century is reported. The constructed models of source zones of the three strongest ($M \geq 8$) earthquakes that occurred in the Chilean subduction zone in 2010, 2014, and 2015 are presented. A comparative analysis of the stress release during these events was carried out. It has been established that the 2010 Maule earthquake could have contributed to the initiation of the 2015 Illapel earthquake.

Keywords: seismic process, Chilean subduction zone, strongest earthquakes, seismotectonic deformations, source zone, migration of earthquakes

DOI: 10.1134/S1028334X22600943

Island arcs and active continental margins, located at the periphery of the Pacific Ocean, are among the most tectonically and seismically active zones on the Earth and are the source of the strongest catastrophic earthquakes. Destructive earthquakes within subduction zones, besides direct macroseismic effects, may lead to tsunami waves. Therefore, one of the most important tasks of both geodynamics and seismology is to study the peculiarities of the seismic process namely in the subduction zones. In this case, it is necessary both to study the dynamics of the seismic process and to identify the possible relationship between strong earthquakes that occur over large distances within the same subduction zone.

Seismic activity in various seismogenic zones, including the zones of subduction, tends to change repeatedly over time. Thus, periods of relative seismic quiescence, when the level of seismic activity decreases, as compared to the average background, are replaced by periods of high seismic activity, when a whole series of very strong earthquakes occur in a particular region of the globe [1]. At the beginning of the 21st century in the Chilean subduction zone, such seismogenic activation was observed. Within the previous decade, three strong tsunamigenic earthquakes occurred in the central and northern parts of Chile: Maule earthquake on February 27, 2010 (Mw = 8.8); the Iquique earthquake on April 1, 2014 (Mw = 8.1); and the Illapel earthquake on September 16, 2015 (Mw = 8.3) [2].

In recent years, a number of works devoted to the study of these earthquakes have been published ([2–4], etc.). However, most studies focus on analyzing only one of the events. In this work, the seismotectonic deformations associated with the strongest earthquakes in Chile in the early 21st century are studied. For this purpose, the data set of satellite geodetic measurements in the Peru–Chilean subduction zone for the period 2009–2015 were analyzed with involvement of seismological information.

The earthquakes studied in this work are characterized by rather similar magnitudes (8.8, 8.1, and 8.3) and a similar type of mechanism, which is a low-angle thrust, dipping toward the continent. Such a structure corresponds to the contractional settings typical of the convergent boundary of lithospheric plates. It should be noted that the same strong seismic events were realized before within sources of the studied earthquakes, and their recurrence periods vary from 63 to 175 years [2] (Fig. 1).

To study the spatial and temporal distribution of deformations of the earth surface caused by the seismogenic activation of the Chilean subduction zone in the early 21st century, three-component time series of satellite geodetic observations on the Chilean coast

[a] *Shirshov Institute of Oceanology, Russian Academy of Sciences, Moscow, 117997 Russia*
[b] *Moscow Institute of Physics and Technology (National Research University), Dolgoprudnyi, Moscow oblast, 141701 Russia*
**e-mail: ir.s.vladimirova@yandex.ru*

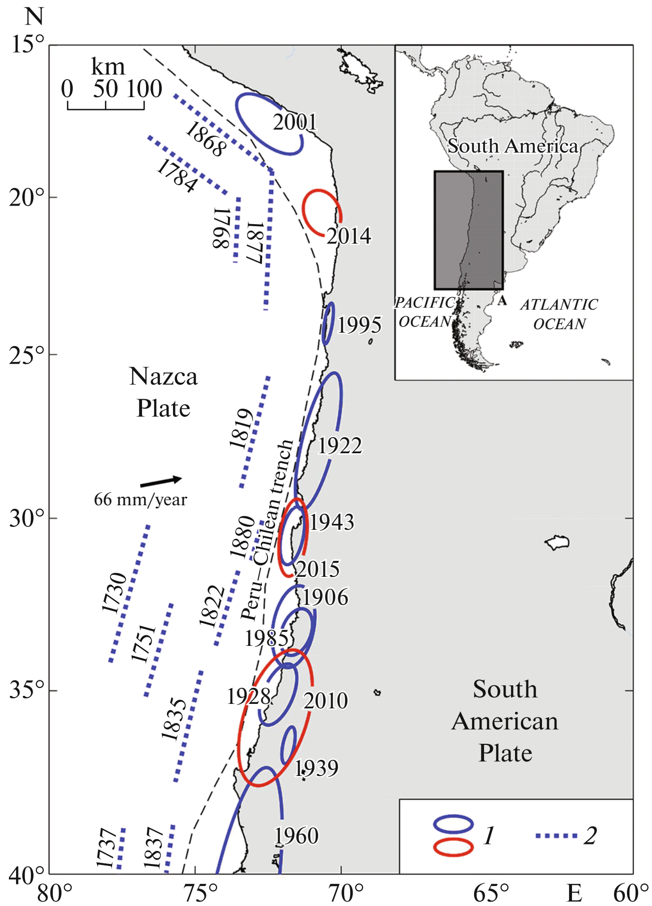

Fig. 1. Location of the source zones of the strongest earthquakes: (*1*) events of the 20th–21st centuries (source zones of the Maule 2010, Iquique 2014, and Illapel 2015 earthquakes are marked in red); (*2*) assumed lengths of seismic ruptures of the strongest historical earthquakes [2–4].

were processed and analyzed. The data were provided by the Nevada Geodetic Observatory [5]. The seismotectonic deformations associated with the strongest earthquakes, Maule 2010, Iquique 2014, and Illapel 2015, were studied on the basis of the analysis of the instantaneous coseismic displacements and variations in the displacement rates of 111 stations over annual intervals. All of the satellite geodetic data presented in this paper are considered relative to the South American Plate.

Variations in the velocities of the modern motions of the earth surface were analyzed. This allows us to reveal the specific features of the geodynamic processes related to the realization of the three strongest earthquakes in the Chilean subduction zone at the beginning of the 21st century. The general codirection of the vector of displacements to the vector of convergence of the plates in 2009–2010 (Fig. 2a) indicates that the entire region studied occurs at the quasi-stationary interseismic stage of the seismic cycle. Similar displacement velocities (30 mm/year in the north and 35–38 mm/year in the south) indicate a relatively equal compression of the continental margin immediately before the occurrence of a series of the strongest earthquakes in 2010–2015. The Maule earthquake of February 27, 2010, triggered postseismic deformations with velocities that exceeded 300 mm/year in the first year after the event (Fig. 2b). A year later, the postseismic displacements decreased threefold, maintaining the oceanward direction (Fig. 2c). In the next three years, a smoother decrease in the values of vectors of the postseismic deformations continued. Thus, two years after the Maule earthquake, the maximum velocities of the postseismic displacements were 75–76 mm/year (Fig. 2d); three years later they decreased to 55 mm/year (Fig. 2e); and four years later they did not exceed 40 mm/year (Fig. 2f). It should be noted that, between the events of 2010 and 2015, postseismic deformations developed in the immediate vicinity of the preparation zone of the Illapel earthquake or even affected its southern margin. During the same time interval, the field of interseismic velocities, recorded north of the region and affected by the Maule earthquake, remains relatively stable. The 2014 Iquique event also caused postseismic deformations, but their intensity was significantly smaller compared to those caused by the 2010 Maule earthquake: the maximum amplitudes of displacements in the first year after the event were 81–83 mm/year (Fig. 2f). An increase in the interseismic displacement velocities by 2–4 mm/year in the source zone of the forthcoming Illapel earthquake may be regarded as a peculiarity for the field of displacement velocities in the period 2014–2015.

To study the features of the deformation processes directly during the Maule 2010, Iquique 2014, and Illapel 2015 earthquakes, models of their sources were constructed. To estimate the geometric parameters of the source zones of the studied events, their aftershocks were identified using the cluster method [6]. The resulting slip distributions are the result of the seismic inversion modeling, which is reduced to the minimum of mismatch between the measured satellite methods and the simulated coseismic displacements:

$$\min_{\mathbf{U}(\mathbf{r}_s)} \sum_i \left| \iint_S \mathbf{G}(\mathbf{r}_i, \mathbf{r}_s)\, \mathbf{U}(\mathbf{r}_s) dS - \mathbf{u}_{\text{obs}}(\mathbf{r}_i) \right|^2,$$

where $\mathbf{u}_{\text{obs}}(\mathbf{r}_i)$ are measured coseismic displacements at the observation point $\mathbf{r}_i$, $\mathbf{G}(\mathbf{r}_i, \mathbf{r}_s)$ are functions of the medium response at the point $\mathbf{r}_i$ on the point dislocation at the point $\mathbf{r}_s$, and $\mathbf{U}(\mathbf{r}_s)$ is a vector of dislocation distributed over the surface of a seismic rupture, S. The response functions $\mathbf{G}(\mathbf{r}_i, \mathbf{r}_s)$ for the spherically symmetric layered model of the Earth are calculated according the procedure described in [7]. The ratios for the dislocation source are given in this work in the form of an uniform slip along a rectangular rupture. The required slip distribution in the source $\mathbf{U}(\mathbf{r}_s)$ is approximated by the finite set of values over noncross-

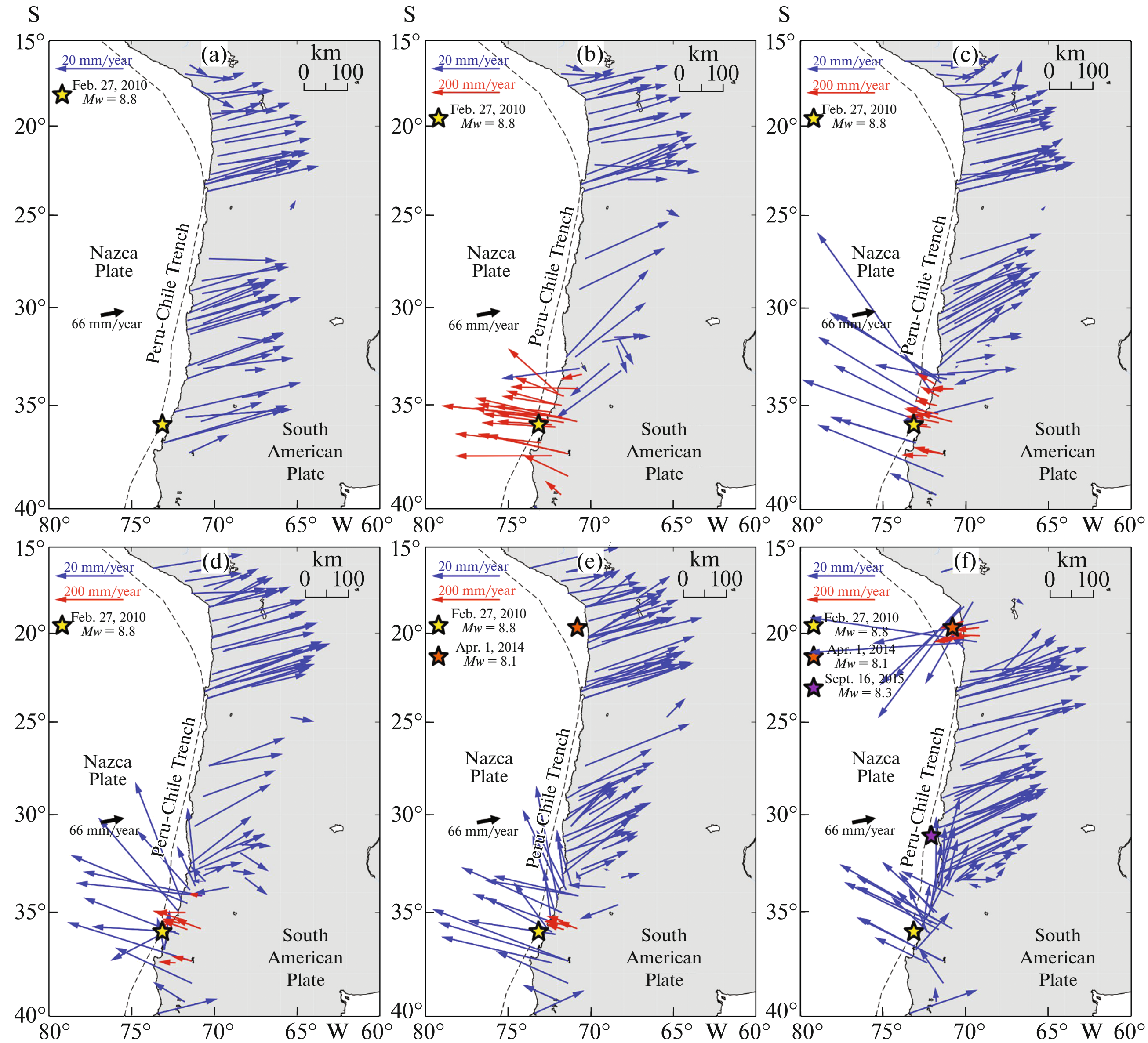

Fig. 2. The velocities of displacements of the network stations for the intervals: (a) February 27, 2009–February 26, 2010; (b) March 2, 2010–March 1, 2011; (c) March 2, 2011–March 1, 2012; (d) March 2, 2012–March 1, 2013; (e) March 2, 2013–March 1, 2014; (f) April 6, 2014–April 6, 2015. The velocities are given relative to the South American lithospheric plate.

ing rectangular discrete elements of the *S* surface; the smoothness condition is superimposed on the desired set of values. Figures 3a–3c illustrate the resulting slip distributions in the sources of the earthquakes studied.

The maximum values of coseismic displacements, recorded during the Maule earthquake, were equal to 4.8 m at the stations near the earthquake epicenter. For the event of 2010, the bilateral development of a seismic rapture was noted. Two zones with a maximum slip of up to 12 m were formed in the southern and central parts of the source zone. Significant displacements of about 10 m are observed in the northern part of the source zone too. The Maule earthquake was accompanied by long-term and intensive aftershock sequence, the main peculiarity of which was the total absence of aftershocks with $M \geq 7.0$: the strongest of them had magnitude 6.9 [4]. The noticeable peculiarity of the development of the aftershock sequence is that the epicenters of aftershocks surround the zones of the maximum displacements in the source. Therefore, during the aftershock activity, relaxation of stresses probably occurred in those parts of the source zone where they remained high after the earthquake.

Two hours after the mainshock, the event with $M_w = 7.4$ occurred at a distance of 300 km from the epicenter of the Maule earthquake; it was character-

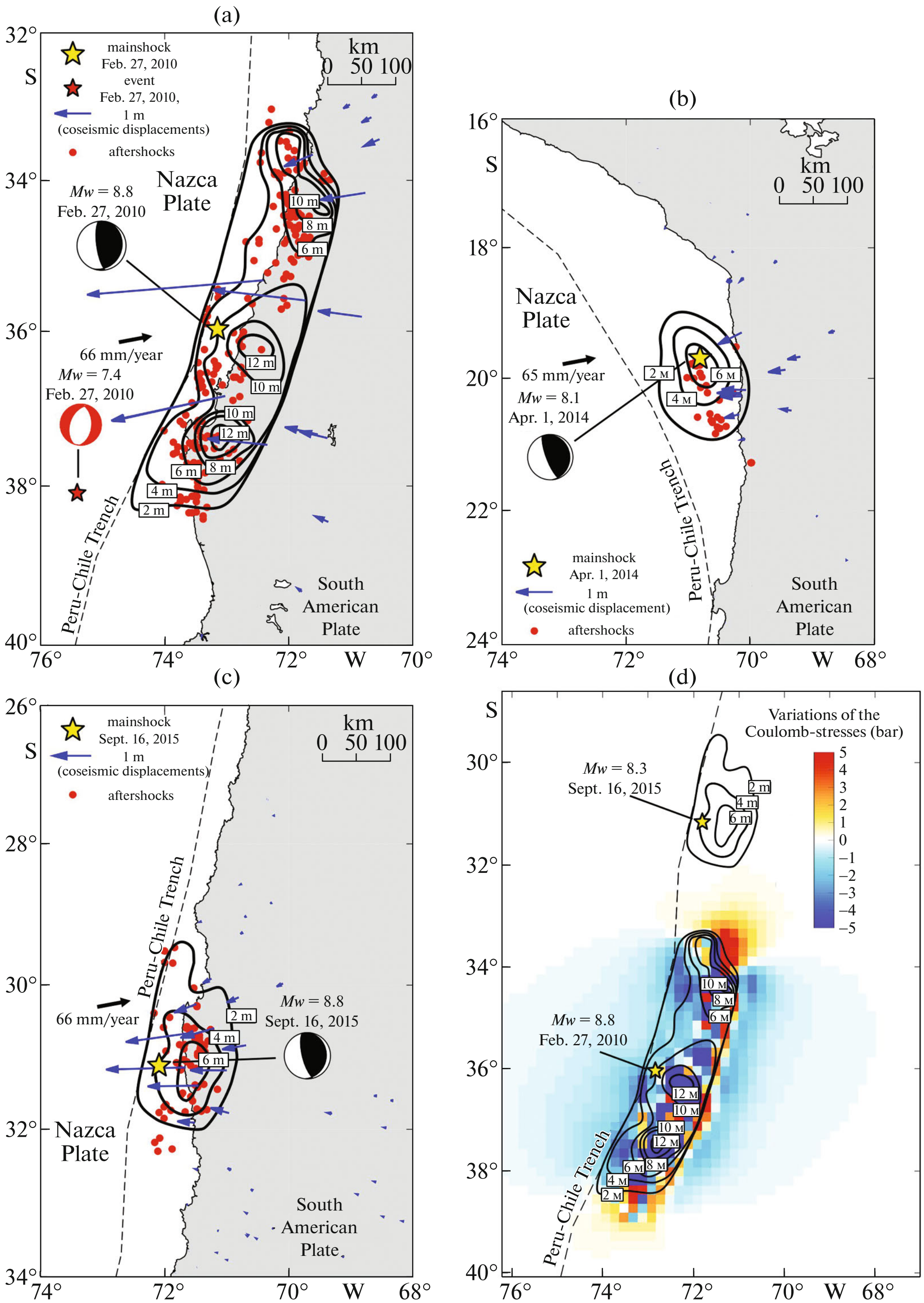

Fig. 3. The source zones and epicenters of aftershocks of the (a) 2010 Maule, (b) 2014 Iquique, and (c) 2015 Illapel earthquakes, and (d) results of calculations of the Coulomb-stress variations caused by the 2010 Maule earthquake. Isolines show the values of slip in the source zones (in meters).

ized by the normal-fault mechanism (Fig. 3a). This event, probably, was initiated by the rapid growth of tensile stresses in the outer trench swell immediately after the Maule earthquake.

The immediate coseismic displacements of the observation points during the Iquique earthquake did not reach even 0.8 m (Fig. 3b), which can be explained by the smaller magnitude of the event in comparison with the 2010 earthquake. A distinctive feature of the 2014 event is the predominantly unidirectional propagation of the rupture, which was less than 200 km long instead of the expected 600 km [3]. Both the zone of significant displacements (up to 6 m) at the earthquake source and the epicenters of aftershocks were generally concentrated to the south of the mainshock. The number of aftershocks registered after this event was rather small. The observed lack of aftershocks can indicate an aseismic creep in the setting of heterogeneous interplate coupling [8]. In other words, during the earthquake, only a part of the assumed source zone ruptured seismically, while the undisturbed zones were displaced aseismically, which may explain the unexpectedly small extent of the seismic source.

The coseismic displacements recorded during the third event, the 2015 Illapel earthquake, reached 2.2 m near the epicenter. The final fault zone was formed as a result of bilateral development of the seismic rupture along the Peru–Chile Trench. The length of the zone where significant seismic displacements occurred was 250 km, and the maximum displacement at the source was up to 6 m. Most of the aftershocks occurred outside the zone of maximum displacements at the source (Fig. 3c), similarly to the case of the Maule earthquake. It allows us to suggest some similarity of the processes of residual stress release after strong earthquakes in the central part of the Chilean subduction zone.

The fact that three strongest events occurred within the same subduction zone within only a six-year time interval allows us to study the immensity and internal connectivity of the seismic process. Works [9–13], etc., gave affirmative answers to the questions about the presence of interrelations of the strong earthquakes occurring over long distances and about the possibility of initiation of some events by others. The migration of earthquake epicenters in different seismically active regions is associated with the transmission of deformations within the Earth through the propagation of wave deformation processes with different velocities [9, 10]. The estimate of the velocity of propagation of deformation waves along the subduction zones and, correspondingly, the velocity of migration of strong earthquakes along the strike of the subduction zone is 50–170 km/year [11]. The distances between the hypocenters of the Maule–Iquique and Iquique–Illapel events are about 1800 and 1300 km, respectively. In this case, the velocity of the propagation of the deformation wave along the Chilean subduction zone should be 430–860 km/year, which is several times higher than the estimations obtained in [11]. At the same time, the distance between the hypocenters of the 2010 Maule and 2015 Illapel earthquakes was less than 550 km. To overcome such a distance in 5.5 years, the deformation wave must propagate at an average velocity of about 100 km/year, which agrees well with the estimations from [11]. Thus, the observed process of earthquake migration in the Chilean subduction zone may be due to the propagation of tectonic stresses, which cause additional stress in the segments of the subduction zone with a high concentration of elastic stresses.

It was also established that distant strong earthquakes can have a decisive influence on the formation of the source of another event at the final stage of its development [12]. At the same time, the next seismic event will occur only in the area where the state of the medium is already close to destruction, and the stress difference, caused by an event that had already occurred, will serve as a trigger mechanism. It was shown in [13] that earthquakes with $M \geq 8$ can impact the seismicity within a radius of 1000 km. The distances between hypocenters of the Maule–Iquique and Iquique–Illapel events (1800 and 1300 km) greatly exceed the specified radius, while the distance between the hypocenters of the Maule–Illapel earthquakes is only 550 km, which means that the source formation zone of the Illapel earthquake occurred within the zone of the influence of the Maule earthquake.

According to the results of experiments on rock deformation, the geological environment is a Coulomb medium, i.e., a brittle medium with internal friction [14]. For such media, the proximity to the critical state, followed by brittle failure, is determined by the Coulomb-stresses, which are the difference between tangential stresses at the rupture surface and the dry friction stress [15].

The possible effect of the Chilean earthquakes on acceleration of the forthcoming next strong earthquake was estimated by calculating the change in the Coulomb-stresses in the fault planes of future earthquakes as a result of realization of the previous earthquake:

$$\Delta\sigma_f = \Delta\tau_B - \mu'(\Delta\sigma_B),$$

where $\Delta\tau_B$ and $\Delta\sigma_B$ are the change in the tangential and normal stresses in the plane of the future earthquake source; $\mu' = \mu(1 - B)$ is the effective friction coefficient; μ is the friction coefficient; and $B \in [0,1]$ is the Scampton coefficient. The Coulomb stresses in this work were calculated with the use of the Coulomb 3 package. As a result of the calculations, no clear relationship between the Maule–Iquique and Iquique–Illapel earthquakes was found. At the same time, it is shown that the Maule earthquake caused Coulomb-stress transfer to the source zone of the future Illapel earthquake (Fig. 3d), which could have brought closer the moment of occurrence of brittle ruptures in this zone. Therefore, the event of 2010 could potentially have contributed to the initiation of the event of 2015.

All of the strongest subduction earthquakes considered above occurred within a short time interval within the same seismogenic zone, characterized by the unity of tectonic conditions. However, the comparative analysis made it possible to reveal a number of significant differences in the development of the deformation processes in the vicinities of their sources. These differences are presumably defined by unique tectonic and geological conditions, typical of the source zone of a particular event. To reveal individual peculiarities of the source formation and relaxation of residual stresses after earthquakes, it seems advisable to model the geodynamic processes occurred in the vicinity of the source zones during pre-seismic and post-seismic periods.

FUNDING

This work was supported by the Russian Science Foundation, project no. 20-17-00140.

CONFLICT OF INTEREST

The author declares that she has no conflicts of interest.

REFERENCES

1. L. M. Balakina and A. G. Moskvina, Izv., Phys. Solid Earth **48** (2), 117–155 (2012).
2. S. A. Ruiz and R. Madariaga, Tectonophysics **733**, 37–56 (2018).
3. T. Lay, H. Yue, E. E. Brodsky, and C. An, Geophys. Rev. Lett. **41**, 3818–3825 (2014).
4. C. Mora-Stock and W. Rabbel, in *The Chilean Earthquake and Tsunami 2010. A Multidisciplinary Study of Mw 8.8, Maule* (WIT PRESS, Boston, 2013), pp. 1–24.
5. G. W. Blewitt, C. Hammond, and C. Kreemer, EOS **99** (2018). https://doi.org/10.1029/2018EO104623
6. V. B. Smirnov, Geofiz. Issled. **10** (2), 7–22 (2009).
7. F. F. Pollitz, Geophys. J. Int. **125**, 1–14 (1996).
8. P. N. Shebalin, I. A. Vorobieva, S. V. Baranov, and V. O. Mikhailov, Dokl. Earth Sci. **498** (1), 423–427 (2021).
9. V. G. Bykov, Geodin. Tektonofiz. **9** (3), 721–754 (2018).
10. A. V. Vikulin, G. M. Vodinchar, V. K. Gusyakov, I. V. Melekestsev, D. R. Akmanova, A. A. Dolgaya, and N. A. Osipova, Vestn. Kamchat. Gos. Tekh. Univ., No. 17, 5–15 (2011).
11. D. L. Anderson, Science **187** (4181), 1077–1079 (1975).
12. A. V. Nikolaev and G. M. Vereshchagina, Dokl. Akad. Nauk SSSR **318** (2), 320–324 (1991).
13. Z. A. Kal'met'eva and F. N. Yudakhin, Dokl. Akad. Nauk **335** (2), 225–231 (1994).
14. Yu. L. Rebetskii, Fiz. Mezomekh. **10** (1), 25–37 (2007).
15. J. R. Rice, in *Physics of the Earth's Interior,* Ed. by A. M. Dziewonski and E. Boschi (North Holland, 1980).

Translated by V. Krutikova